

**Paper No.
MCI36**



**Suppression of anodic kinetics of stainless steels
by natural seawater biofilms**

M. EASHWAR

CSIR – Central Electrochemical Research Institute, Karaikudi – 630006, Tamil Nadu, India
eashwar1960@gmail.com

**A. Lakshman Kumar, G. Sreedhar, S. Vengatesan,
R. Ananth and V. Prabhu**

CSIR – Central Electrochemical Research Institute, Karaikudi – 630006, Tamil Nadu, India

ABSTRACT

The effect of biofilms on the anodic kinetics of three stainless steels, viz. UNS S31600, S44660 and N08367 in quiescent flowing natural seawater was investigated. Potentiodynamic anodic polarization showed two distinct passive regimes emerging with biofilm development. In the lower passive region near the ennobled open-circuit potential, biofilms produced dramatic decrease of anodic current densities ($i < 10^{-4}$) accompanied by an increase of the breakdown potential by over 0.2 V for alloy S31600. Biofilms, however, led to significant broadening of the transpassive region on all the three alloys tested. Further, for alloys S44660 and N08367, biofilms altered the second passive region and amplified the peak current densities therein. These seemingly undesired effects, nonetheless, were detected far beyond practical realms. Potentiostatic current–time curves for alloy N08367 further confirmed the suppression of anodic kinetics in the lower passive region. Evans diagrams constructed from actual polarization curves provide fundamentally important insights that passivity promotion can be independent of microbially enhanced cathodic kinetics.

Keywords: stainless steels; seawater; microbial biofilms; anodic kinetics; passivity; extracellular material.

NIGIS * CORCON 2017 * 17-20 September * Mumbai, India

Copyright 2017 by NIGIS. The material presented and the views expressed in this paper are solely those of the author(s) and do not necessarily by NIGIS.

INTRODUCTION

Biofilms grow ubiquitously on metallic surfaces immersed in seawater. With particular reference to stainless steels (SSs), biofilms leads to an ennobling of the open circuit potential (OCP), besides accelerating the cathodic kinetics in a dramatic manner¹⁻⁴. Implications for the biofilm-enhanced cathodic kinetics are (a) increased current requirement for cathodic protection^{5,6}, (b) increased propagation rates of localized attack of the less corrosion-resistant alloys⁷⁻⁹, and (c) accelerated corrosion of anodic materials in galvanic contact with SSs^{10,11}.

In the classical illustration of SS immersed in natural seawater¹²⁻¹⁵, it is generally presumed that anodic polarization is virtually unaffected and that the interfacial phenomenon is controlled entirely by cathodic kinetics. This implies that the passive current density would stay unchanged during biofilm development. It is also usually presumed that biofilms make the alloys more vulnerable to localized corrosion initiation by pushing the OCP closer to the breakdown potential (E_{bd}). Up till now, surprisingly, hardly any research has been conducted on the anodic kinetics of SSs during biofilm development in seawater. More often in the literature, the significance of anodic kinetics has been dismissed based on assumptions rather than on the strength of experimental data.

Mansfeld¹⁶ and Little¹⁷ raised an interesting question of the mechanism by which the less corrosion-resistant SSs such as UNS S30400 and S31600 can reach OCP far beyond theoretical E_{bd} regimes and yet stay without corrosion initiation for long periods of time. Although the possibility of 'inhibitor' production by marine biofilms has been mentioned frequently in literature¹⁸⁻²¹, the influence that biofilms can have on the passive current density has never been methodically evaluated. Thus, the objective of this work is to provide the first insights into the effect of seawater biofilms on the anodic kinetics and the passive regimes of SSs.

EXPERIMENTAL PROCEDURE

STAINLESS STEELS INVESTIGATED

Three grades of SSs were used, all purchased from Metal Samples Company, Munford, AL (USA) in the form of 150 x 100 x 1.1 mm coupons. Alloy UNS S31600 (type 316 stainless steel) was a natural choice in view of its global marine application and also because of its inherent vulnerability to corrosion. Alloys S44660 (Seacure) and N08367 (AL-6XN) represented marine grade stainless steels with superior corrosion resistance. The nominal compositions of the alloys are listed in Table 1. The coupons had a glass-beaded finish.

Table 1: Stainless steels used, their designations and nominal compositions.

Alloy name	UNS number	Elemental composition (wt %)											
		C	Co	Cr	Cu	Fe	Mn	Mo	N	Ni	P	Si	Ti
SS-316	S31600	0.01	0.21	16.4	0.33	68.9	1.59	2.02	0.04	10.07	0.02	0.41	0.00
Seacure	S44660	0.02	0.00	27.5	0.15	65.99	0.33	3.63	0.02	1.84	0.02	0.37	0.13
AL-6XN	N08367	0.01	0.00	20.83	0.24	48.31	0.34	6.06	0.21	23.63	0.02	0.35	0.00

NIGIS * CORCON 2017 * 17-20 September * Mumbai, India

Copyright 2017 by NIGIS. The material presented and the views expressed in this paper are solely those of the author(s) and do not necessarily by NIGIS.

SEAWATER IMMERSION TESTS

The experimental site (Mandapam coast, Bay of Bengal, Indian Ocean; 9° 16' N, 79° 9' E) and the method of seawater immersion in this work were the same as in our recent investigations^{4,21}. Succinctly, exposures were setup in the laboratory employing a gravity-feed and overflow method where freshly sampled seawater flowed gently ($\sim 5 \text{ l h}^{-1}$) from 100 l reservoir tanks into 30 l test troughs. The ambience in the laboratory corresponded to very low light conditions, thus excluding an effect of illumination on passivity^{21,22,23}. The alloy coupons were immersed edge-on to the flow and to two-thirds of their length such as to exclude galvanic effects. The physicochemical characteristics of seawater were periodically monitored as per standard methods²⁴

BIOFILM CHARACTERIZATION

Epifluorescent microscopy was used for documenting the early stages of biofilm formation (12 to 15 d immersion) with S31600 as the sample alloy. Coupons were fixed in 3% buffered glutaraldehyde for 4 h and then stained for 15 minutes with acridine orange. A Nikon-Eclipse epifluorescence microscope Model Ni-U was employed and images were captured on to a computer using Nikon NIS-Elements software. Biofilms were also viewed by field emission scanning electron microscopy (FESEM, Carl Zeiss SUPRA 55VP). Samples were fixed in 2.5% glutaraldehyde (2.5% v/v 0.1 M phosphate buffer, pH 7.4) for 4 h, followed by a dehydration sequence in acetone, critical point drying and gold sputtering. Here, early as well as mature stages of biofilms were examined.

At the end of the immersion, the biofilms were collected by carefully swabbing the coupons with cotton wool and dried at ambient room temperature. They were powdered, homogeneously mixed in a 1:10 ratio with potassium bromide, and made into a pellet using a hydraulic pressing machine. Fourier Transform Infra-Red (FTIR) spectra of the samples were recorded on a Bruker Tensor 27 Spectrometer in the frequency range from 4000 to 400 cm^{-1} with a resolution of 0.125 cm^{-1} .

ELECTROCHEMICAL MEASUREMENTS

Periodic measurement of the OCP of the alloys was made using a high impedance voltmeter (FLUKE 28 II) together with a saturated calomel electrode (SCE). An array of 5 SCEs was used, and these were periodically calibrated as described earlier¹¹ to ensure a variation within 5 mV of one another. Potentiodynamic anodic polarization of biofilmed coupons was made at the end of the test (65 d) on GAMRY Reference-600 Electrochemistry Workstation with a computer interface using REF-600 14037 software. A scan rate of 0.16 mV sec^{-1} was employed, proceeding from the equilibrium OCP to a range appropriate for the study of passivity. Unexposed controls were also correspondingly scanned, both anodically and cathodically, after the bare coupons equilibrated in 0.22 μm (Millipore) filtered seawater for ~ 1 h.

Measurements were also made of current-time relationship for alloy N08367 using the GAMRY Workstation in the potentiostatic mode. Anodic and cathodic current transients at OCP were recorded every day in 30 minute slots, employing 5 replicate coupons each time.

NIGIS * CORCON 2017 * 17-20 September * Mumbai, India

Copyright 2017 by NIGIS. The material presented and the views expressed in this paper are solely those of the author(s) and do not necessarily by NIGIS.

RESULTS AND DISCUSSION

WATER CHARACTERISTICS AND OPEN-CIRCUIT POTENTIALS

On average, the coastal seawater had a temperature of 29.5° C, a salinity of 33.7 psu, dissolved oxygen level of 5.7 mg l⁻¹ and a pH 8.22. Fig. 1 shows OCP evolution with time for 5 coupons each of the three SSs immersed in natural seawater, illustrating typical ennobling during biofilm growth. The OCP approached a plateau by 30 d and remained fairly unchanged until 65 d.

The epifluorescence images Fig. 2a through 2f document the early stages of biofilm growth, showing variety of microorganisms ranging from a scatter of individual bacterial cells to filamentous

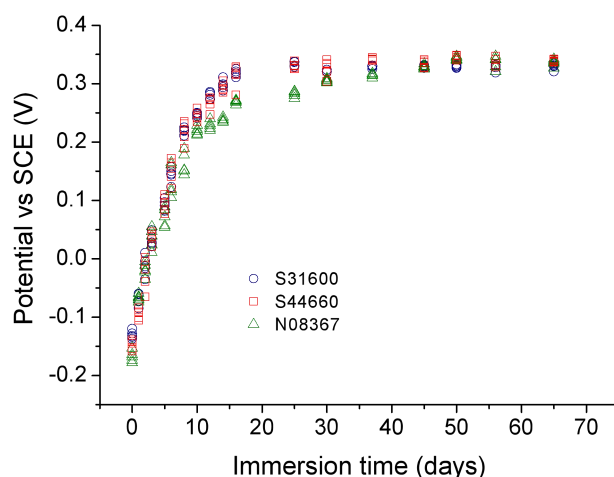


Figure 1: The evolution of OCP with time for 5 coupons each of S31600, S44660 and N08367 immersed in natural seawater.

BIOFILM CHARACTERISTICS

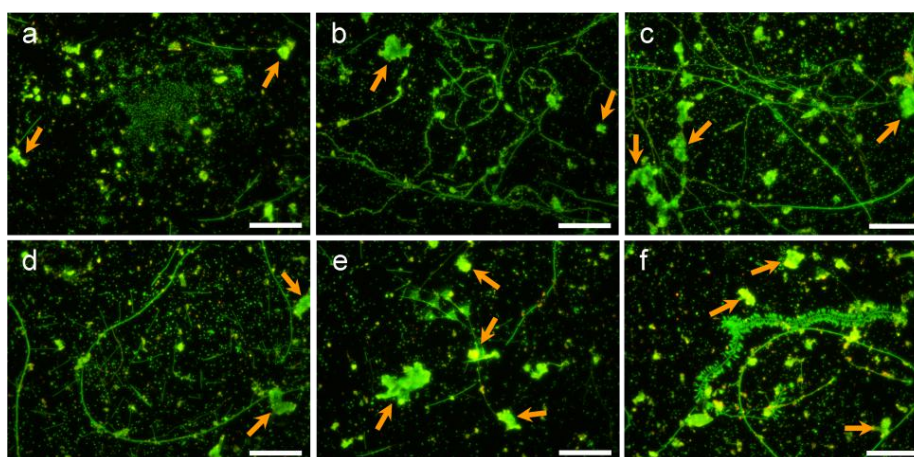


Figure 2a to 2f: Epifluorescence images of biofilm development on S31600 during early biofilm growth in natural seawater, showing the diversity of organisms and the presence of extracellular microbial material (indicated by arrows). Scale bars denote 25 μ m on all images.

NIGIS * CORCON 2017 * 17-20 September * Mumbai, India

Copyright 2017 by NIGIS. The material presented and the views expressed in this paper are solely those of the author(s) and do not necessarily by NIGIS.

organisms, chains of bacteria, individual large rods, fungal cells and protozoans. The arrows in the images indicate extracellular material embedded in the biofilm matrix. Images of biofilm documented by FESEM are shown in Figures 3a through 3d. The early biofilm (Fig. 3a and 3b) can be seen to consist of chains of bacteria and protozoans similar to those in epifluorescence images in Fig. 2b and 2f respectively. The FESEM images in Figure 3c and 3d document later stages of biofilm growth taken at higher magnification. These images provide evidence of copious formation of extracellular material by the biofilm microorganisms.

In Fig. 4, the FTIR spectra of biofilms exhibit a good level of consistency. The broad twin peaks at 3470 and 3400 cm^{-1} represent O-H and N-H stretching, respectively. The N-H out-of-plane bending appearing at 1620 cm^{-1} can be assigned to amides. The peaks at 1080 and 1150 cm^{-1} correspond, respectively, to C-O and P=O stretching.

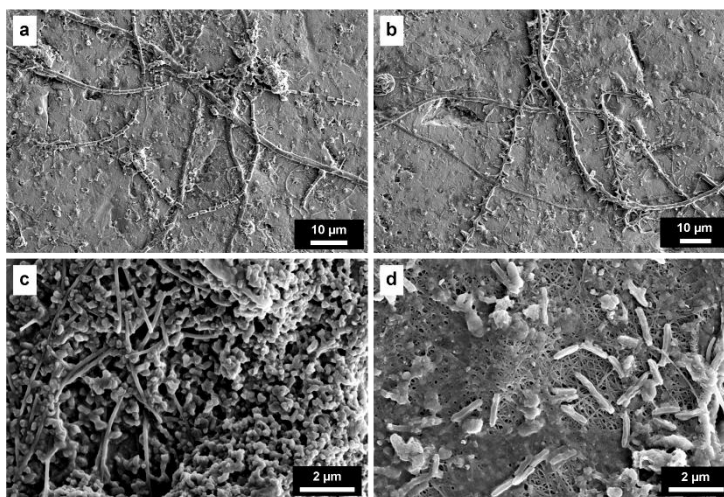


Figure 3a to 3d: FESEM images of biofilm development on S31600 during early (a, b) and later (c, d) stages of immersion in natural seawater. Copious formation of extracellular material is clearly visible in image 3d.

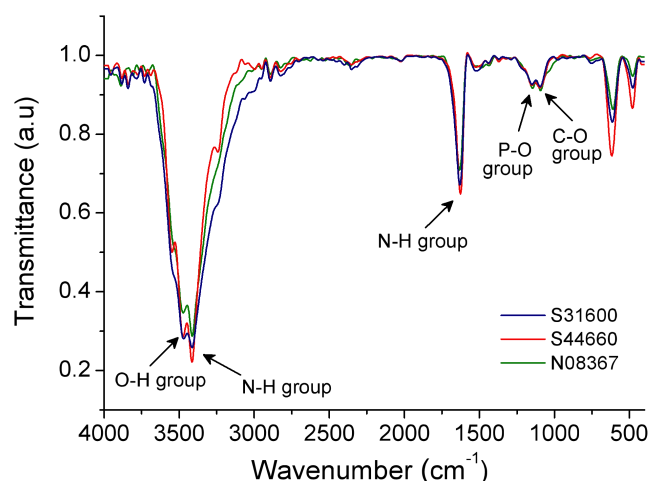


Figure 4: FTIR spectra of biofilms formed on the three stainless steels in natural seawater illustrating the presence of various functional groups.

NIGIS * CORCON 2017 * 17-20 September * Mumbai, India

Copyright 2017 by NIGIS. The material presented and the views expressed in this paper are solely those of the author(s) and do not necessarily by NIGIS.

POTENTIODYNAMIC ANODIC POLARIZATION CURVES

Fig. 5 depicts the anodic polarization behaviour of the three SSs, derived from multiple coupons, before and after biofilm formation in seawater. The polarization scans for S31600 in Fig. 5a show a number of interesting features. Firstly, the anodic current densities near the OCP were dramatically lower for the biofilmed coupons than those for the controls. Thus, the mean current densities at potentials 0.05 V nobler to the OCP were $0.18 \pm 0.027 \mu\text{A cm}^{-2}$ and $0.47 \pm 0.10 \mu\text{A cm}^{-2}$ for the biofilmed and controls, respectively, with a statistically high level of significance ($n = 5$; $F = 35.66$; $p = 3.33 \times 10^{-4}$). Secondly, the anodic scans for biofilmed coupons presented a subtle change in slope ~ 0.05 V nobler to the OCP, indicated by an arrow in Fig. 5a (mean = 54.8 ± 3.27 mV). We have assigned the realm below this position (slope = 163.6 ± 8.85 mV decade $^{-1}$) as the lower passive region and the one above (slope = 101 ± 4.06 mV decade $^{-1}$) as the transpassive region. Also, the character of the lower passive and transpassive regions for the biofilmed coupons was radically different from that for the controls, with a distinctly unusual slant, contrary to the depiction in conceptual Evans diagrams¹²⁻¹⁵. The difference in slopes in the transpassive region between the controls (196.2 ± 5.49 mV decade $^{-1}$) and biofilmed coupons (101 ± 4.06 mV decade $^{-1}$) was extraordinarily significant ($F = 903$; $p = 1.63 \times 10^{-9}$). One further noteworthy feature was a marked increase of E_{bd} for biofilmed coupons [0.582 ± 0.025 V (SCE)] over the controls [0.33 ± 0.057 V (SCE)], which was again statistically quite substantial ($p = 1.84 \times 10^{-5}$).

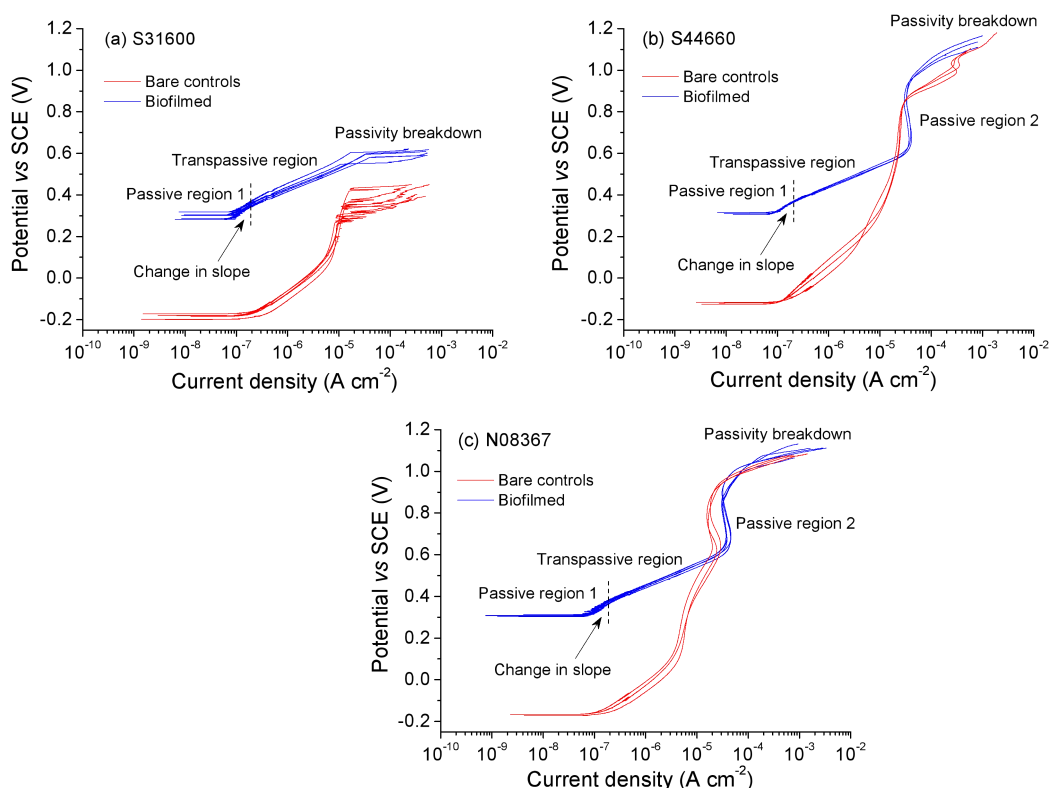


Figure 5a to 5c: Suites of potentiodynamic anodic polarization scans for bare and biofilmed coupons of the stainless steels (a) S31600, (b) S44660 and (c) N08367 in natural seawater.

NIGIS * CORCON 2017 * 17-20 September * Mumbai, India

Copyright 2017 by NIGIS. The material presented and the views expressed in this paper are solely those of the author(s) and do not necessarily by NIGIS.

The anodic polarization scans for S44660 and N08367 in Fig. 5b and 5c show several characteristics comparable to those for S31600 including a subtle change in slope, denoted by arrows, separating the lower passive and transpassive regions. The location of this split from the OCP was almost identical to that for S31600, being 52.46 ± 3.43 mV and 53.92 ± 7.54 , respectively, for S44660 and N08367. At 0.4 V (SCE), the anodic current densities for both alloys were exceptionally smaller on biofilmed coupons, compared to the controls ($F > 132.2$; $p < 3.25 \times 10^{-4}$). Furthermore, a second passive region appeared around 0.6 V (SCE) at much higher anodic current densities. For both alloys, the peak current densities at the beginning of the second passive region were somewhat larger for biofilmed coupons than for controls, with relatively smaller significance ($F = < 1.8$; $p > 0.1$). For alloy S44660, biofilms enhanced the span of the second passive region as well as the E_{bd} , while these were comparatively unchanged on N08367.

POTENTIOSTATIC CURRENT-TIME BEHAVIOUR

Fig. 6a illustrates the current-time behaviour of N08367 at the open-circuit. The diminution of anodic currents with biofilm development is consistent with the potentiodynamic data. The figure also shows that the cathodic currents increased by 20 d immersion and thereafter stayed almost unchanged. The anodic current spikes in Fig. 6b for an individual sample plotted over 25 minute slots with immersion time suggest that transpassive events can happen during early periods of immersion even on a highly corrosion-resistant alloy like N08367 and that biofilms effectively smothered this behaviour with time.

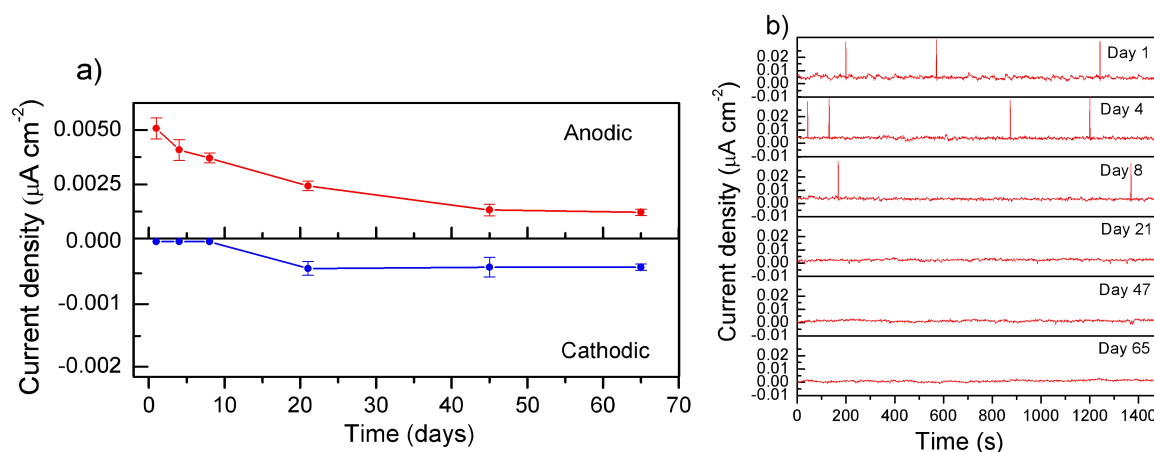


Figure 6: Current-time behaviour of UNS N08367 at open-circuit in natural seawater. (a) means with SDs for 5 samples; (b) behaviour of an individual sample.

EVANS DIAGRAMS FROM ACTUAL POLARIZATION CURVES

Cathodic polarization curves were obtained on a separate set of N08367 coupons immersed in natural seawater for 65 days, and these were superimposed on the corresponding anodic curves previously shown in Fig. 5c. Note from these curves in Figure 7 an appreciable enhancement of cathodic kinetics, quite typical of biofilm development. The so-obtained Evans diagram from actual polarization curves differs radically from the theoretical¹²⁻¹⁵, and provides an important implication that the suppression of anodic kinetics can be independent of an enhancement of cathodic kinetics.

NIGIS * CORCON 2017 * 17-20 September * Mumbai, India

Copyright 2017 by NIGIS. The material presented and the views expressed in this paper are solely those of the author(s) and do not necessarily by NIGIS.

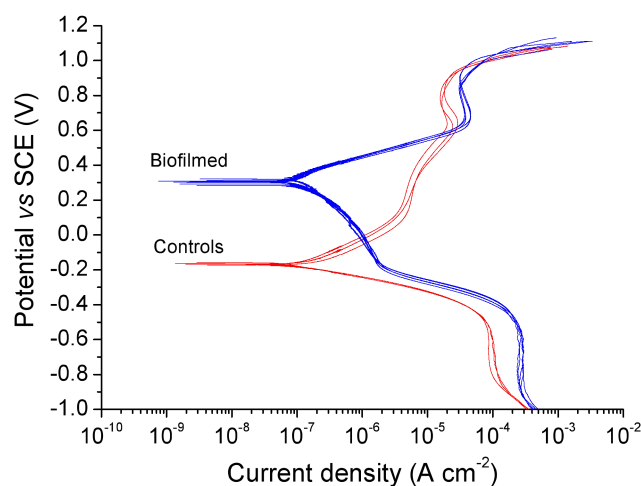


Figure 7: Evans diagrams for bare and biofilmed UNS N08367 constructed from actual polarization curves obtained on UNS N08367 in seawater.

The present data constitute the first suite of well-founded anodic polarization scans for SSs in natural seawater. These results provide strong evidence of a significant suppression of anodic kinetics of SSs by seawater biofilms. The results also bring to light several interesting features as illustrated in Fig. 3, including the occurrence of a lower passive region close to the ennobled OCP, which has hitherto remained undetected. The data clearly imply that there can be no such thing as ‘unchanging anodic kinetics’ or ‘static film’, provoking the conception of passive film ageing and growth^{25,26,27}. The data also provide conclusive evidence that the anodic kinetics of SSs tends to change, leading to promotion of passivity with immersion and ageing. In other words, the data clearly illustrate that the passive film reacts to the environment it is in, evolving with time and the action of biofilms. The phenomenon appears most likely to be through microbially produced extracellular substances (Fig. 4) that possess exceptional passivity-promoting properties²⁸. This work provides a perfect answer to the query by Mansfeld¹⁶ and Little¹⁷, explaining the continued existence of SS passivity far beyond theoretical breakdown limits. It is also believed that this work provides fresh insights to our understanding of SS behaviour under marine conditions.

CONCLUSIONS

Natural seawater biofilms produced statistically quite significant suppression of anodic kinetics on alloys S31600, S44660 and N08367. For the less corrosion-resistant S31600, there was an increase in E_{bd} by over 0.2 V. The enhancement was most likely due to microbial extracellular material. Evans diagrams generated from actual polarization curves provided fundamentally new insights that passivity promotion and enhanced cathodic kinetics can occur concomitantly.

ACKNOWLEDGMENTS

This work was funded by the Council of Scientific and Industrial Research, New Delhi, India under MULTIFUN (grant number CSC-0101F).

NIGIS * CORCON 2017 * 17-20 September * Mumbai, India

Copyright 2017 by NIGIS. The material presented and the views expressed in this paper are solely those of the author(s) and do not necessarily by NIGIS.

REFERENCES

1. A. Mollica and A. Trevis, "The influence of microbiological film on stainless steels in natural seawater," V. Romanovsky, Ed. In: Proceedings of the 4th International Congress on Marine Corrosion and Fouling, 1976, Centre de Recherches et D'Etudes Oceanographiques, Boulogne, France, pp. 351–365.
2. S.C. Dexter, "Microbiologically influenced corrosion," in Corrosion: Fundamentals, Testing, and Protection, vol. 13A, S.D. Cramer, B.S. Covino Jr, Eds. Philadelphia: ASM press, 2003, pp. 398–416.
3. M. Faimali, et al., "Evidence of enzymatic catalysis of oxygen reduction on stainless steels under marine biofilm," Biofouling, vol. 27, pp. 375–384, 2011.
4. M. Eashwar, A. Lakshman Kumar, R. Hariharasuthan and G. Sreedhar, "The relationship between alloying elements and biologically produced ennoblement in natural waters," Biofouling, vol. 31, pp. 433–442, 2015.
5. R. Johnsen and E. Bardal, "Cathodic properties of different stainless steel in natural seawater," Corrosion, vol. 41, pp. 296–302, 1985.
6. B. Little, P. Wagner and D. Duquette, "Microbiologically induced increase in corrosion current density of stainless steel under cathodic protection," Corrosion, vol. 44, pp. 270–274, 1988.
7. P. Gallagher, R.E. Malpas and E.B. Shone, "Corrosion of stainless steels in natural, transported and artificial seawater," Brit. Corros. J., vol. 23, pp. 229–233, 1988.
8. H.J. Zhang and S.C. Dexter, "Effect of biofilms on crevice corrosion of stainless steels in coastal seawater," Corrosion, vol. 51, pp. 56–66, 1995.
9. L.L. Machuca, et al., "Effect of oxygen and biofilm on crevice corrosion of UNS S31803 and UNS N08825 in natural seawater," Corros. Sci., vol. 67, pp. 242–255, 2013.
10. S.C. Dexter and J.P. LaFontaine, "Effect of natural marine biofilms of galvanic corrosion," Corrosion, vol. 54, pp. 851–861, 1998.
11. M. Eashwar, et al., "Cathodic behaviour of stainless steel in coastal Indian seawater: calcareous deposits overwhelm biofilms," Biofouling, vol. 25, pp. 191–201, 2009.
12. V. Scotto, R. Di Cintio and G. Marcenaro, "The influence of marine aerobic microbial film on stainless steel corrosion behaviour," Corros. Sci., vol. 25, pp. 185–194, 1985.
13. S.C. Dexter and G.Y. Gao, "Effect of seawater biofilms on corrosion potential and oxygen reduction of stainless steel," Corrosion, vol. 44, pp. 717–723, 1988.
14. A. Mollica, A. Trevis, E. Traverso, G. Ventura and R. Dellepine, "Cathodic performance of stainless steel in natural seawater as a function of microorganism settlement and temperature," Corrosion, vol. 45, pp. 48–56, 1989.

NIGIS * CORCON 2017 * 17-20 September * Mumbai, India

Copyright 2017 by NIGIS. The material presented and the views expressed in this paper are solely those of the author(s) and do not necessarily by NIGIS.

15. B. Little and F. Mansfeld, "Passivity of stainless steels in natural water," F. Mansfeld, A. Asphahani, H. Bohn and R.M. Latanision, Eds. In: Proceedings of HH Uhlig symposium, 1995, Pennington (NJ), The Electrochemical Society, pp. 42–55.
16. F. Mansfeld, "The interaction of bacteria and metal surfaces," *Electrochim. Acta*, vol. 52, pp. 7670–7680, 2007.
17. B. Little, J.S. Lee and R.I. Ray, "The influence of marine biofilm on corrosion: a concise review," *Electrochim. Acta.*, vol. 54, pp. 2–7, 2008.
18. S.C. Dexter, "Role of microfouling organisms in marine corrosion," *Biofouling*, vol. 7, pp. 97–127, 1993.
19. M. Eashwar and S. Maruthamuthu, "Biologically produced ennoblement: ecological perspectives and a hypothetical model," *Biofouling*, vol. 8, pp. 203–213, 1995.
20. J. Landoulsi, K.E. Cooksey and V. Dupres, "Review: interactions between diatoms and stainless steel: focus on biofouling and biocorrosion," *Biofouling*, vol. 27, pp. 1105–1124, 2011.
21. M. Eashwar, G. Sreedhar, A. Lakshman Kumar, R. Hariharasuthan and J. Kennedy, "The enrichment of surface passive film on stainless steel during biofilm development in coastal seawater," *Biofouling*, vol. 31, pp. 511–525, 2015.
22. D.D. Macdonald and D.F. Heaney, "Effect of variable intensity ultraviolet radiation on passivity breakdown of AISI type 304 stainless steel," *Corros. Sci.*, vol. 42, pp. 1779–1799, 2000.
23. M. Eashwar, G. Subramanian, S. Palanichamy and G. Rajagopal, "The influence of sunlight on the localized corrosion of UNS S31600 in natural seawater," *Biofouling*, vol. 27, pp. 837–849, 2011.
24. J.D.H. Strickland and T.R. Parsons, *A Practical Handbook of Seawater Analysis*, Ottawa: Fisheries Research Board of Canada, 1972.
25. C. Compere, D. Festy and P. Jaffre, "Aging of type 316L stainless steel in seawater: relationship between open circuit potential, exposure time and pitting potential," *Corros. Sci.*, vol. 52, pp. 496–501, 1996.
26. D.D. Macdonald, "Passivity: the key to our metal based civilization," *Pure Appl. Chem.*, vol. 71, pp. 951–978, 1999.
27. C.O.A. Olsson and D. Landolt, "Passive film on stainless steels: chemistry, structure and growth" *Electrochim. Acta*, vol. 48, pp. 1093–1104, 2003.
28. M. Moradi, Z. Song and X. Tao, "Introducing a novel bacterium, *Vibrio neocaledonicus*, with the highest corrosion inhibition efficiency," *Electrochem. Commun.*, vol. 51, pp. 64–68, 2015.

NIGIS * CORCON 2017 * 17-20 September * Mumbai, India

Copyright 2017 by NIGIS. The material presented and the views expressed in this paper are solely those of the author(s) and do not necessarily by NIGIS.